

# Statistical Learning for Heterogeneous Treatment Effects: Pretraining, Prognosis, and Prediction

Maximilian Schuessler

[maxsc@stanford.edu](mailto:maxsc@stanford.edu)

Erik Sverdrup

[erik.sverdrup@monash.edu](mailto:erik.sverdrup@monash.edu)

Robert Tibshirani

[tibs@stanford.edu](mailto:tibs@stanford.edu)

May 2025

## Abstract

Robust estimation of heterogeneous treatment effects is a fundamental challenge for optimal decision-making in domains ranging from personalized medicine to educational policy. In recent years, predictive machine learning has emerged as a valuable toolbox for causal estimation, enabling more flexible effect estimation. However, accurately estimating conditional average treatment effects (CATE) remains a major challenge, particularly in the presence of many covariates. In this article, we propose pretraining strategies that leverages a phenomenon in real-world applications: factors that are *prognostic* of the outcome are frequently also *predictive* of treatment effect heterogeneity. In medicine, for example, components of the same biological signaling pathways frequently influence both baseline risk and treatment response. Specifically, we demonstrate our approach within the *R*-learner framework, which estimates the CATE by solving individual prediction problems based on a residualized loss. We use this structure to incorporate “side information” and develop models that can exploit synergies between risk prediction and causal effect estimation. In settings where these synergies are present, this cross-task learning enables more accurate signal detection: yields lower estimation error, reduced false discovery rates, and higher power for detecting heterogeneity.

## 1 Introduction

For many applications, from personalized medicine to educational policies, understanding treatment effects beyond global averages is critical for optimal decision-making and treatment prioritization. For example, a cancer treatment may show average benefits for a patient population, yet individual responses can vary widely

among patients (Tomasik et al. 2024). In the presence of such heterogeneity, the average may be composed of individuals with large, moderate, and negative treatment effects (Kravitz et al. 2004). Those with minimal benefit or harm are better off receiving no or alternative treatments. This explains why in medicine and other high-stakes settings, relying solely on average treatment effects (ATE) can lead to suboptimal decisions—potentially harming some individuals or, incorrectly, withholding treatment from those who could benefit. To advance precision medicine, researchers and practitioners are, therefore, interested in developing as highly personalized treatment recommendations as possible (Kosorok & Laber 2019). One common strategy for deriving personalized treatment policies is to use a risk-based approach, where individuals prone to poor outcomes receive treatment first (Kent et al. 2016, 2020). An alternative approach is to prioritize individuals based on their treatment benefit (Manski 2004, Wager & Athey 2018).

In settings with expected differential treatment responses, knowing each unit’s individual treatment effect (ITE) enables the design of personalized treatment policies, prioritization rules, and helps prevent under- or over-treatment. In practice, however, the ITE is not point-identified (Imbens & Rubin 2015). A common strategy to obtain more granular treatment effects is to estimate the conditional average treatment effect (CATE), which is still an average treatment effect but conditional on a set of covariates. Conditioning on more covariates makes this average more specific, potentially revealing subgroups with treatment effects that differ significantly from the overall average.

With the widespread availability of large-scale observational data, researchers now have access to rich data environments that offer the potential to estimate the conditional average treatment effects for increasingly granular subgroups. Simultaneously, machine learning has emerged as a useful toolbox, offering several advantages for CATE estimation (Athey & Imbens 2016). A large body of work has made considerable progress towards more flexible estimation, e.g. by using the lasso (Imai & Ratkovic 2013), boosting (Powers et al. 2018), multivariate adaptive regression (Powers et al. 2018), neural networks (Shalit et al. 2017), and random forests (Wager & Athey 2018), to name just a handful of approaches. Moreover, these models can be flexibly integrated into metalearners (Kennedy 2023, Künzel et al. 2019, Morzywolek et al. 2023, Nie & Wager 2021, van der Laan et al. 2024) that decompose the exercise of effect estimation into separate prediction tasks. This has enhanced the role of statistical learning for CATE estimation in recent years.

Beyond more flexible estimation, automated CATE models offer a principled and objective way of identifying and reporting subgroups that drive heterogeneous treatment responses (Athey et al. 2019). This provides a remedy to a more traditional approaches in which practitioners need to define relevant subgroups *a priori*. Moreover, it mitigates practices similar to *p*-hacking, where possible subgroups are re-

peatedly searched until a putative signal for heterogeneity is found. Especially in areas like genetics, where treatment heterogeneity is often the results of complex interactions, such manual approaches are not scalable and become easily impractical.

Despite these advances, there remains a fundamental statistical difficulty in CATE estimation (Kennedy et al. 2024). Identifying heterogeneous treatment effects is especially challenging when sample sizes are limited (e.g., in rare diseases) or when effects are diffuse and involve complex interactions. Identifying effect modifiers then often resembles the task of finding a “needle in a haystack”. For example, in settings with  $p = 10$  binary covariates, there are already  $2^{10} = 1024$  possible subgroups that could explain heterogeneity. The challenge grows in high-dimensional settings like gene expression data, where  $p$  can be as large as, or even exceed  $n$ . In those settings, low power, overfitting and high variance are concerns that complicate estimating the CATE (Hastie et al. 2009, Powers et al. 2018, Candes et al. 2018).

Low sample sizes and high-dimensional data are common challenges in medical settings. For instance, clinical trials increasingly include more covariates (e.g., from molecular data), while their sample sizes have not kept pace. As a result, there is an urgent need for methods that improve upon traditional approaches to CATE estimation. Ignatiadis & Huber (2021) suggest mitigating these challenges by leveraging domain knowledge and hidden “side information” in the data—for example, to derive data-driven weights for hypothesis testing. In a similar vein, Fortney et al. (2015) and Dobriban et al. (2015) show how prior information on disease-related gene loci may help elucidate loci for longevity due to their existing overlap. Seemingly unrelated disease loci can predict treatment responses across multiple conditions. These examples highlight that real-world datasets in biomedicine, though often characterized by a low signal-to-noise ratio, are rich in connections and structures. These might involve risk measures that serve as surrogates for treatment effects and help uncover effect modifiers. In predictive settings, statistical learning methods that incorporate weights from related tasks—commonly known as transfer learning—have gained significant attention over the past decades (Argyriou et al. 2006, Craig et al. 2024, Gu et al. 2024, Obozinski et al. 2010, Zou 2006, Li et al. 2022). Harnessing putative “side information” for heterogeneous treatment effects, bears a considerable potential, but requires statistical learning strategies that can synergize seemingly distinct prediction tasks for CATE estimation.

In this article, we use the term “pretraining” as an umbrella term to denote various statistical learning procedures that enable a sequential transfer of information from one (or multiple) prediction model(s) to another. Depending on the architecture of each model, this can take the form of using the active set from a lasso to derive penalty factors for the second model (adaptive lasso), performing weighted feature sampling based on feature importance in tree-based learners or transferring weights to a neural network.

We leverage recent advances in statistical learning for formulating the CATE estimation as a causal loss minimization objective. We focus our exposition on the  $R$ -learner and exploit a common phenomenon in real-world settings: factors that are prognostic of the mean outcome are frequently predictive of the treatment effect. We claim that in settings in which covariates have this dual role of being prognostic *and* predictive, we can improve CATE estimation by synergizing predictive learning tasks. We refer to this approach as “pretraining the  $R$ -learner”. In addition, we showcase how this approach can be generalized for various linear and non-linear learners and their statistical learning properties. In a nutshell:

- (a) We propose a pretraining strategy that goes beyond treating the mean outcome function as a mere nuisance parameter in the  $R$ -learner framework: we leverage the shared support between prognostic and predictive factors for conditional average treatment effect estimation.
- (b) The goal of this approach is threefold: first, increase the accuracy of CATE estimation by exploiting synergies between seemingly independent prediction tasks; second, improve the support recovery of effect modifiers/interacting effects; and third, gain more insights about the putative existence of shared support between prognostic and predictive factors when estimating the CATE.
- (c) To demonstrate this approach, we develop a suite of estimation frameworks using the lasso-based  $R$ -learner ( $R$ -lasso) and non-parametric models. We also demonstrate how this approach can be extended to non-linear settings using basis function expansions and random forests.

## 2 Leveraging Side Information for Heterogeneous Treatment Effect Estimation

Let  $\{Y_i(0), Y_i(1)\}$  denote potential outcomes in the control and treatment state (Imbens & Rubin 2015). Suppose  $n$  units of observation resulting in tuples  $\{Y_i, W_i, X_i\}_{i=1}^n$ , where  $Y_i = Y_i(W_i)$  corresponds the  $i$ -th unit’s realized outcome,  $W_i = \{0, 1\}$  denotes the treatment assignment, and  $X_i \in \mathcal{X}$  are individual-level features, where  $\mathcal{X}$  is some potentially large  $p$ -dimensional feature space. We make the following assumptions.

**Assumption 1.** (Unconfoundedness). Conditional on a set of observed covariates  $X_i$ , treatment assignment  $W_i$  is independent of  $Y_i$ ,

$$\{Y_i(0), Y_i(1)\} \perp\!\!\!\perp W_i \mid X_i.$$

**Assumption 2.** (Positivity). The propensity score  $e(x) = \mathbb{P}[W_i = 1 \mid X_i = x]$ , which defines the probability of exposure to treatment conditional on covariates, is

bounded away from 0 and 1. There exists an  $\eta > 0$  such that

$$\eta \leq e(x) \leq 1 - \eta \text{ for all } x \in \mathcal{X}.$$

**Remark 1.** To simplify notation, we use the symbol  $X_i$  to refer to both potential confounders, treatment effect modifiers, etc. We emphasize this distinction when it matters.

The ideal clinical decision making quantity is the  $i$ -th unit's treatment effect,  $Y_i(1) - Y_i(0)$ . By the fundamental problem of causal inference, this quantity, however, is not point identified because each unit  $i$  can either receive treatment or not. In order to gain insight into personalized treatment responses it is helpful to instead shift attention to conditional average treatment effects (CATE), defined as  $\tau(x) = \mathbb{E}[Y_i(1) - Y_i(0) | X_i = x]$ . We denote the mean conditional potential outcome in arm  $w$  by  $\mu_{(w)}(x) = \mathbb{E}[Y_i(w) | X_i = x]$ . Given Assumption 1,  $\mu_{(w)}(x) = \mathbb{E}[Y_i | X_i = x, W_i = w]$ , and the CATE is identified by

$$\tau(x) = \mathbb{E}[Y_i | X_i = x, W_i = 1] - \mathbb{E}[Y_i | X_i = x, W_i = 0]. \quad (1)$$

An immediate strategy to obtain estimates of CATE via this identity is to estimate  $\mu_{(0)}(X_i)$  and  $\mu_{(1)}(X_i)$  via predictive machine learning algorithms fitted separately on each treatment arm, followed by estimating the CATEs through their plug-in difference  $\hat{\tau}(X_i) = \hat{\mu}_{(1)}(X_i) - \hat{\mu}_{(0)}(X_i)$ . This approach is usually referred to as the  $T$ -learner (Künzel et al. 2019).

A drawback of this simple direct approach is regularization bias due to, for example, treatment imbalance (Künzel et al. 2019). Recent advances have produced an array of improvements to this approach by decomposing prediction tasks into tailored loss functions that directly target the CATE (e.g., Foster & Syrgkanis (2023), Kennedy (2023), Künzel et al. (2019), Morzywolek et al. (2023), Nie & Wager (2021), van der Laan et al. (2024)). The goal of these approaches is to strip out confounding and baseline effects and then focus on the CATE target parameter. Common in these loss-based approaches are nuisance components that we might leverage for the final CATE goal. In particular, the  $R$ -learner (Nie & Wager 2021) leverages Robinson's transformation (Robins 2004, Robinson 1988) to express the CATE function as

$$\tau(\cdot) = \operatorname{argmin}_{\tau} \left\{ \mathbb{E} \left[ \left[ (Y_i - m(X_i)) - (W_i - e(X_i))\tau(X_i) \right]^2 \right] \right\}, \quad (2)$$

where  $m(x) = \mathbb{E}[Y_i | X_i = x]$  is the mean conditional outcomes marginalized over treatment. To estimate CATE via this approach, we form suitable cross-fit/sample-split estimates  $\hat{m}(X_i)$  and  $\hat{e}(X_i)$  of the mean outcomes and propensity scores, then

plug them into the corresponding empirical loss<sup>1</sup>, which we minimize over some chosen CATE function class:

$$\hat{\tau}(\cdot) = \operatorname{argmin}_{\tau} \left\{ \frac{1}{n} \sum_{i=1}^n \left[ (Y_i - \hat{m}(X_i)) - (W_i - \hat{e}(X_i))\tau(X_i) \right]^2 \right\}. \quad (3)$$

This loss function satisfies an oracle property that roughly guarantees that as long as  $\hat{m}(X_i)$  and  $\hat{e}(X_i)$  are estimated reasonably well, we get similar performance to as if we had access to true  $m(X_i)$  and  $e(X_i)$ . This empirical  $R$ -loss yields a tunable causal loss,

$$\hat{L}_n = \frac{1}{n} \sum_{i=1}^n \left[ (Y_i - \hat{m}(X_i)) - (W_i - \hat{e}(X_i))\hat{\tau}(X_i) \right]^2, \quad (4)$$

which allows us to tune hyperparameters in the learner for  $\tau(x)$ . If certain features in the support of  $m(X_i)$  are also predictive of  $\tau(X_i)$ , then the loss of this CATE function should ideally reflect the benefits from leveraging prognostic side information in a data-driven way.

Another way of expressing the CATE via a data-dependent loss with similar oracle guarantees is the *DR*-learner (Kennedy 2023) that leverages Robins et al. (1994)'s augmented inverse-propensity weighted scores to fit the CATE via the following pseudo-outcome regression

$$\hat{\tau}(\cdot) = \operatorname{argmin}_{\tau} \left\{ \sum_{i=1}^n \left[ \left( \hat{\mu}_{(0)}(X_i) + \hat{\mu}_{(1)}(X_i) + \frac{W_i - \hat{e}(X_i)}{\hat{e}(X_i)(1 - \hat{e}(X_i))} (Y_i - \hat{\mu}_{(W_i)}(X_i)) \right) - \tau(X_i) \right]^2 \right\}. \quad (5)$$

One particularly useful ingredient in this loss is the model for the conditional mean in the absence of treatment,  $\hat{\mu}_{(0)}(X_i)$ . If features that are predictive of baseline outcomes also matter for treatment benefits, then sharing information between  $\hat{\mu}_{(0)}(X_i)$  and  $\hat{\tau}(X_i)$  might be advantageous in estimating the CATE. For statistical reasons that we discuss shortly and brevity, we restrict our study to exploring leveraging the *R*-learner to share information between marginalized outcomes  $m(X_i)$  and the CATE. However, note that the same logic holds for the *DR*-learner. For a general discussion and comparison of these orthogonal losses for CATE estimation, we refer to Morzywolek et al. (2023).

## 2.1 Shared Support between Prognostic and Predictive Factors

There are many ways in which information can be shared between two statistical tasks to yield a better outcome. In this study, we explore mechanisms that leverage

---

<sup>1</sup>Whenever an estimated quantity, such as  $\hat{m}(X_i)$ , enters the right-hand side of an expression, we abstain from resorting to additional notation and maintain the convention that the  $i$ -th predictions are constructed without using the  $i$ -th unit for estimation, such as with, for example, cross-fold estimation.

the “shared support” of two prediction tasks. We define shared support as a setting in which two or more prediction tasks operate over a common active feature space—that is, a subset of input variables that are informative and utilized across tasks. While this requires overlap in the predictors, the targets may differ.

A common observation in medicine and other fields is that factors that are prognostic of an outcome are also predictive of treatment response, i.e. there is a overlap in the support of features that are relevant to solve the objective function for the mean outcome function  $m(X_i)$  and those for the CATE function  $\tau(X_i)$ . Equation 6 expresses this phenomenon in an easy toy based on a linear model. The covariate  $X_{i1}$  is simply *prognostic* of the outcome  $Y_i$  (in the absence of the treatment);  $X_{i3}$  is *predictive* as it interacts with the treatment. Finally,  $X_{i2}$  is both prognostic and predictive.

$$Y_i = \beta_0 + X_{i1}\beta_1 + X_{i2}\beta_2 + W_i\tau(X_i) + \varepsilon_i \quad (6)$$

$$\tau(X_i) = \theta_0 + X_{i2}\theta_2 + X_{i3}\theta_3 \quad (7)$$

**Definition 1.** (Prognostic Factor). A prognostic factor is any covariate or combination of covariates that contains information about the likelihood an outcome, independent of any treatment assignment ([Ballman 2015](#), [National Cancer Institute 2025b](#)).

**Definition 2.** (Predictive Factor). A predictive factor is any covariate or combination of covariates that contains information about the likelihood of the treatment effect  $\tau(X_i)$ . A predictive factor interacts with the treatment. This interaction can be *quantitative*, where both groups (with and without the prognostic factor) benefit from the treatment but at varying degree; or *qualitative*, that is either the group with or without the predictive factor derives a positive effect from the treatment, but not both ([Ballman 2015](#), [National Cancer Institute 2025a](#)).

## Pretraining Strategies for the R-Learner

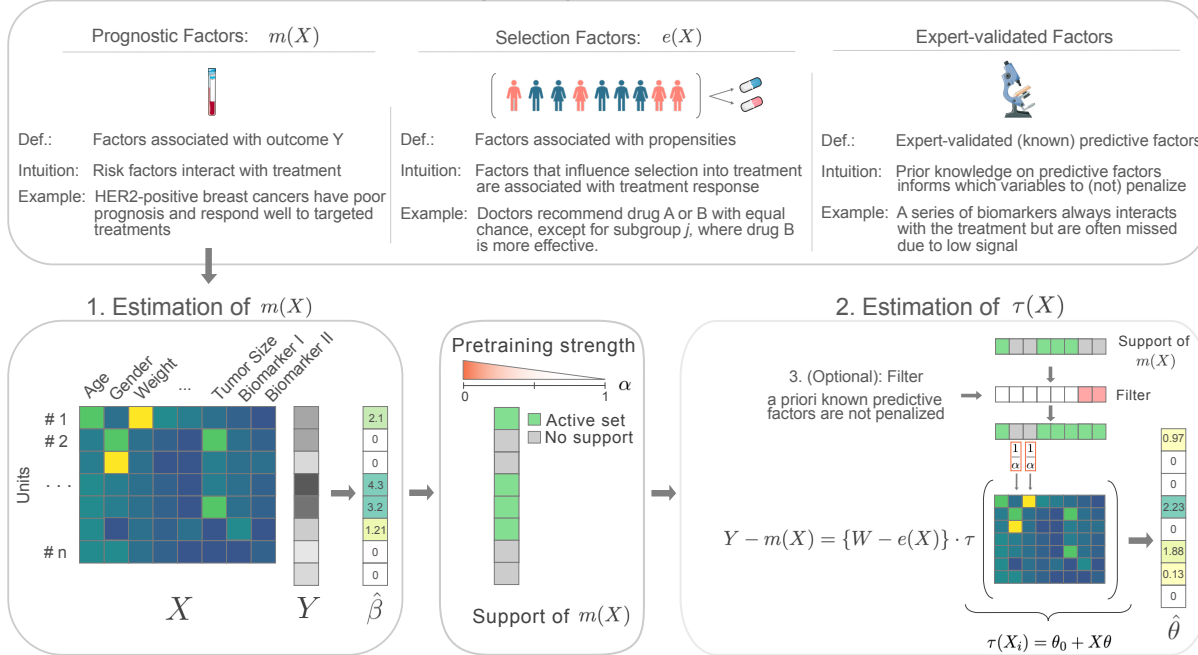


**Figure 1: Overview of the Pretrained R-learner.** The figure shows the step-wise procedure of the R-learner with the mean outcome function and the CATE. The upper panel shows different pretraining strategies. The lower panels illustrate how these pretraining approaches are integrated into the R-learner using the mean outcome function as example. The active set for the mean outcome model (left panel) is used for pretraining to inform the estimation of the conditional average treatment effect (CATE) model. Here, gender, weight, and biomarker II are not in the support of the mean outcome model (middle panel) and get penalized at  $1/\alpha$  when estimating the CATE model (right panel). Optionally, previously known, expert-validated predictive factors are exempt from any penalties. For example, biomarker II is a known to be predictive (and thus protected from any penalties *a priori*), but not in the active set of the mean outcome model. Age, tumor size, and biomarker I are in the supports of both models, and do not get penalized through pretraining. Icons from Servier Medical Art, licensed under CC BY 4.0, <https://creativecommons.org/licenses/by/4.0/>.

A classic example in medicine for the presence of this joint support is Human Epidermal Growth Factor Receptor 2 (HER2): individuals with a breast cancer of this type, which occurs in approximately 20% of all cases, have a higher risk of relapse and shorter overall survival (Slamon et al. 1987). HER2 expression is associated with increased resistance to chemotherapy (Slamon et al. 2001), while enhancing sensitivity to specific subclasses of therapies targeted against HER2 (Hudis 2007). Thus, HER2 is both a prognostic factor for survival outcomes  $Y_i$  and predictive of the treatment effect  $\tau(X_i)$ . In addition to single biomarkers, there is an increasing

number of composite biomarkers such as gene signatures that determine risk and treatment response in oncology (Chapuy et al. 2018, Alizadeh et al. 2000, Rueda et al. 2019).

The overlap of predictive and prognostic factor also plays a role in psychiatry and cardiology: patients with depression have a higher risk and poorer outcomes for cardio-vascular diseases (CVD) (Lichtman et al. 2014). Furthermore, patients who suffer from depression are at higher risk for medication non-adherence, which can decrease the effectiveness of CVD medications such as statins and anti-hypertensive treatments (DiMatteo et al. 2000, Carney & Freedland 2017). Finally, the phenomenon of shared support is likely to extend to many other disciplines outside medicine. Athey et al. (2025) demonstrate that baseline responses are easier to estimate than treatment effect and leverage this for enhanced causal predictions to target behavioral nudges. In education, for example, school-specific characteristics, such as learning environments, not only predict students' overall educational performance, but also often modify the effects of educational interventions (Yeager et al. 2019).

## 2.2 Side Information from Selection Factors

It is possible to extend our concept of pretraining to the propensity score function in observational settings where treatment assignment is the function of some covariates. Suppose clinicians tend to recommend a treatment to patients in an age group where they believe it is most effective. These patients will have high treatment propensity. If clinicians are generally correct, then the same covariates driving propensity will also predict treatment benefit. Cohen & DeRubeis (2018) discuss the role of prognostic, predictive and selection factors in the context of depression. Selection factors also play an important role in phase-II and phase-III cancer trials, where investigators choose one (“physician’s choice”) among many treatment options in the control arm (Modi et al. 2022, Ribas et al. 2015).

**Definition 3.** (Selection Factor). A *selection factor* is any pre-exposure covariate which contains information about the likelihood of treatment assignment.

Pretraining on selection factors might be also relevant in other areas for research such as education. There is large body of research examining the effect of learning interventions or college admission on outcomes (e.g. future income). In this example, selection factors such as socio-economic status, motivation, belief’s about one’s future, and health might be strong effect modifiers (Yeager et al. 2016).

### 3 Using the Lasso to Leverage Prognostic Side Information

In order to instantiate an  $R$ -learner that leverages shared support, we need learners for the mean conditional outcome function and CATE function amendable to this support-sharing task. One tractable solution is to leverage an adaptive lasso for the CATE function where the differential shrinkage parameters are set through the lasso active set solution for the mean conditional outcome function. For exposition it is helpful to first consider regularized high-dimensional linear models. Suitable featurizations of the covariate matrix (Hastie et al. 2009) allow us to extend this approach to non-linear settings as revisited in section 4. We start out by assuming a randomized controlled trial setting where the propensity scores are known and omit this estimation task. We start by fitting  $m(X_i)$  with the lasso

$$m(X_i) = \beta_0 + \sum_{j=1}^p X_{ij}\beta_j, \quad (8)$$

$$\hat{\beta} = \operatorname{argmin}_{\beta} \left\{ \sum_{i=1}^n \left[ Y_i - m(X_i) \right]^2 + \lambda_1 \sum_{j=1}^p |\beta_j| \right\},$$

where  $\lambda_1$  is a regularization parameter that minimizes the cross-validated MSE. In addition to the estimated model coefficients  $\hat{\beta}$ , the lasso yields an active set of features with nonzero coefficients. If some of these coefficients are not part of the active set, then as argued in Section 2.1, they might be less useful for estimating the CATE. In the next step we incorporate information from this active set by estimating  $\tau(X_i)$  via an adaptive lasso using (3)

$$\tau(X_i) = \theta_0 + \sum_{j=1}^p X_{ij}\theta_j, \quad (9)$$

$$\hat{\theta} = \operatorname{argmin}_{\theta} \left\{ \frac{1}{n} \sum_{i=1}^n \left[ (Y_i - \hat{m}(X_i)) - (W_i - \hat{e}(X_i))\tau(X_i) \right]^2 + \lambda_2 \sum_{j=1}^p w_j |\theta_j| \right\}.$$

Here, the regularization parameter  $\lambda_2$  applies equally to each feature, but the weights  $w_j$  control the relative regularization strength depending on the estimated conditional mean model (8) support,

$$w_j = \begin{cases} 1/\alpha, & \text{if } \hat{\beta}_j = 0 \\ 1, & \text{if } \hat{\beta}_j \neq 0. \end{cases} \quad (10)$$

The additional tuning parameter  $\alpha$  controls how much differential regularization to place on factors that are not estimated to be prognostic, and we refer to this as

the “pretraining strength” (Craig et al. 2024). As we lower  $\alpha$  from 1 (no penalty) to 0 (penalty towards  $\infty$ ), the strength of the penalty factor increases until the feature is effectively removed from the model. Using the  $R$ -loss allows us to treat  $\alpha$  and thereby the pretraining strength as a tunable hyperparameter depending on the size of the overlap between  $m(X_i)$  and  $\tau(X_i)$ . Figure Figure 2 shows the  $R$ -loss on the training set and mean squared error (MSE) on the test set for varying  $\alpha$  in a simulation setting with partially shared support. The  $R$ -loss serves as a reliable loss for tuning, as both errors reach their minimum at  $\alpha = 0.375$ .

In empirical settings in which the assumption that high risk (prognosis) entails high treatment benefit proves wrong (for empirical examples see Earle et al. (2008) or Weeks et al. (1998)), we expect the  $R$ -loss to favor  $\alpha$ ’s closer to 1, removing the pretraining effect. Algorithm 1 summarizes the pretrained  $R$ -lasso.

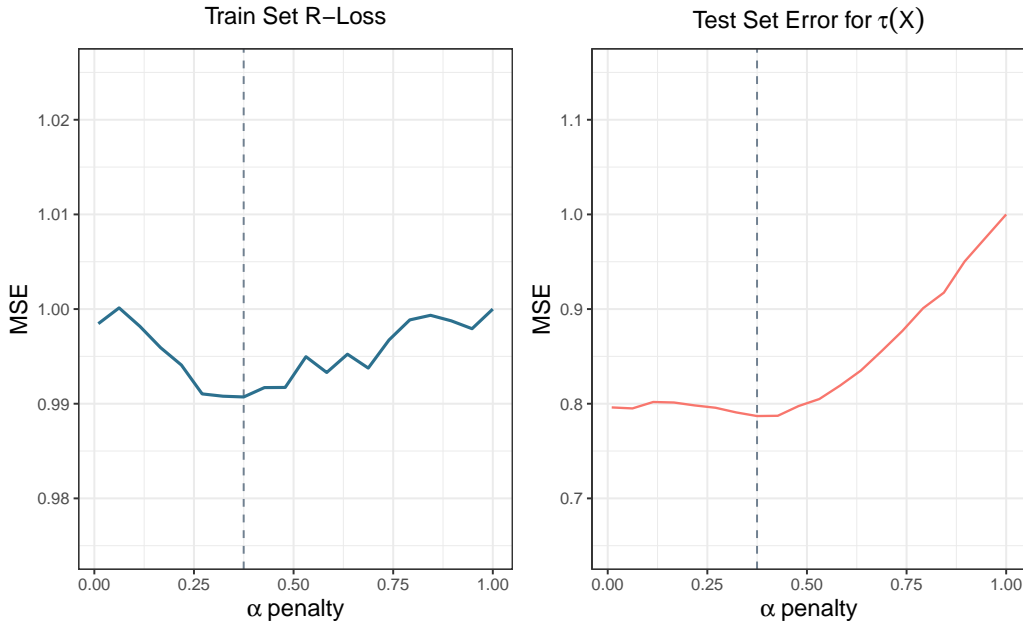


**Figure 2: Hyperparameter Tuning Using the  $R$ -Loss.** The figure shows the median performance of the  $R$ -lasso in terms of  $R$ -loss on the training set and MSE on the test set in a linear setting with  $n = 500$ ,  $p = 150$ ,  $SNR = 2$ , an active set of size  $|S| = \frac{p}{3}$  and for 5000 repetitions. The dashed vertical lines show the  $\alpha$ s for which the train set  $R$ -loss and test set MSE are minimized.

**Remark 2.** We can employ a similar strategy in the  $DR$ -learner (5) using its nuisance parameters for pretraining. While pretraining based on the conditional outcome model for the control arm  $\mu_{(0)}(X_i)$  is appealing, it has one disadvantage: depending on the fraction of treated units, we will have less data at our disposition. Moreover, pretraining using  $m(X_i)$  has the potential to pick up sig-

nal that stems from  $\tau(X_i)$  given that under Assumption 1 we have that  $m(X_i) = \mu_{(0)}(X_i) + e(X_i)\tau(X_i)$ . This provides a potential safeguard against penalizing predictive factors that are not prognostic when there is little to no overlap between the two types of covariates.

---

**Algorithm 1 : Pretraining the *R*-learner Using the Lasso**


---

**Input:** Data  $\{Y_i, X_i, W_i\}_{i=1}^n$ , grid of tuning parameters  $\{\alpha \in (0, 1], \lambda_2\}$ .

1. Construct cross-fit estimates of the mean outcome function  $m(X_i)$  with the lasso.

$$m(X_i) = \beta_0 + \sum_{j=1}^p X_{ij}\beta_j,$$

$$\hat{\beta} = \operatorname{argmin}_{\beta} \left\{ \sum_{i=1}^n \left[ Y_i - m(X_i) \right]^2 + \lambda_1 \sum_{j=1}^p |\beta_j| \right\}.$$

2. Construct feature-specific penalty factors  $w_j$  using estimates  $\hat{\beta}$  and  $\alpha$ .

$$w_j = \begin{cases} 1/\alpha, & \text{if } \hat{\beta}_j = 0 \\ 1, & \text{if } \hat{\beta}_j \neq 0. \end{cases}$$

3. Set the propensity scores  $e(X_i)$

**if** unknown **then**

Construct cross-fit estimates of  $e(X_i)$  using a logistic lasso.

**else**

Set  $\hat{e}(X_i)$  to the known randomization probabilities.

**end if**

4. Fit  $\tau(X_i)$  using  $w_j$ -weighted lasso with common regularization  $\lambda_2$ .

$$\tau(X_i) = \theta_0 + \sum_{j=1}^p X_{ij}\theta_j,$$

$$\hat{\theta} = \operatorname{argmin}_{\theta} \left\{ \frac{1}{n} \sum_{i=1}^n \left[ (Y_i - \hat{m}(X_i)) - (W_i - \hat{e}(X_i))\tau(X_i) \right]^2 + \lambda_2 \sum_{j=1}^p w_j |\theta_j| \right\}.$$

**Return:** the estimated  $\hat{\tau}(X_i)$  that minimizes the cross-validated *R*-loss (4).

---

### 3.1 Simulations under Varying Shared Support Sizes

In a first step, we hypothesized that using the active support from the lasso model for  $m(X_i)$  as pretraining information would improve the estimation of  $\tau(X_i)$ . The simulation here aims to test the ability of the pretrained  $R$ -lasso to improve on CATE estimation as we increase the size of the joint support. For ease of exposition, we demonstrate our approach in an easy toy example of a linear setting and generate data as follows. For more complex settings, we refer to [subsection 3.2](#) as well as [section 4](#). All simulations are conducted in the statistical software R ([R Core Team 2024](#)) and implemented using the packages `glmnet` ([Friedman et al. 2010](#)) and `rlearner` ([Nie & Wager 2021](#)).

Our experiments are conducted assuming a randomized trial setting. In this first experiment, we suppose  $n$  units, for each we are given a binary treatment assignment  $W_i \sim \text{Binom}(e(X_i))$ , with  $e(X_i) = 0.5$ ,  $p$  covariates  $X_i \sim \mathcal{N}(0, 1)^p$  and an outcome  $Y_i = \mu_i + \varepsilon_i$ . We define  $\mu_i = \beta_0 + \sum_{j=1}^n X_{ij}\beta_j + W_i \cdot \tau(X_i)$ , with  $\tau(X_i) = \theta_0 + \sum_{j=1}^n X_{ij}\theta_j$ , where  $\beta_j \sim U(0.5, 1)$ ,  $\theta_j \sim U(1, 2)$ , and  $\varepsilon_i \sim \mathcal{N}\left(0, \frac{\text{Var}(\mu)}{SNR}\right)$ . We then introduce some sparsity and limit the size of the active support for  $m(X_i)$  and  $\tau(X_i)$  to  $p/3$ , respectively. We start out with a fully disjoint support where, which we gradually increase until the support is fully shared, i.e. equal to  $p/3$ . We evaluate performance in terms of expected mean-squared error (MSE)  $\frac{1}{n} \sum_{i=1}^n [\tau(X_i) - \hat{\tau}(X_i)]^2$ , which we normalize by the median MSE of the baseline  $R$ -lasso.

In our first experiment, we looked at the effect of pretraining the  $R$ -lasso in the two extreme cases, where the support is either fully disjoint or fully shared. Figure 3 shows the performance of the pretrained  $R$ -lasso in comparison to the baseline  $R$ -lasso in both settings and with different pretraining strengths (upper panel). Panel **b** shows the evolution of performance as the shared support increases fully disjoint to fully joint support. In the absence of any overlap, pretraining shows no effect. With increasing shared support, the pretrained  $R$ -lasso achieves lower MSE, especially under strong pretraining (low  $\alpha$ ).

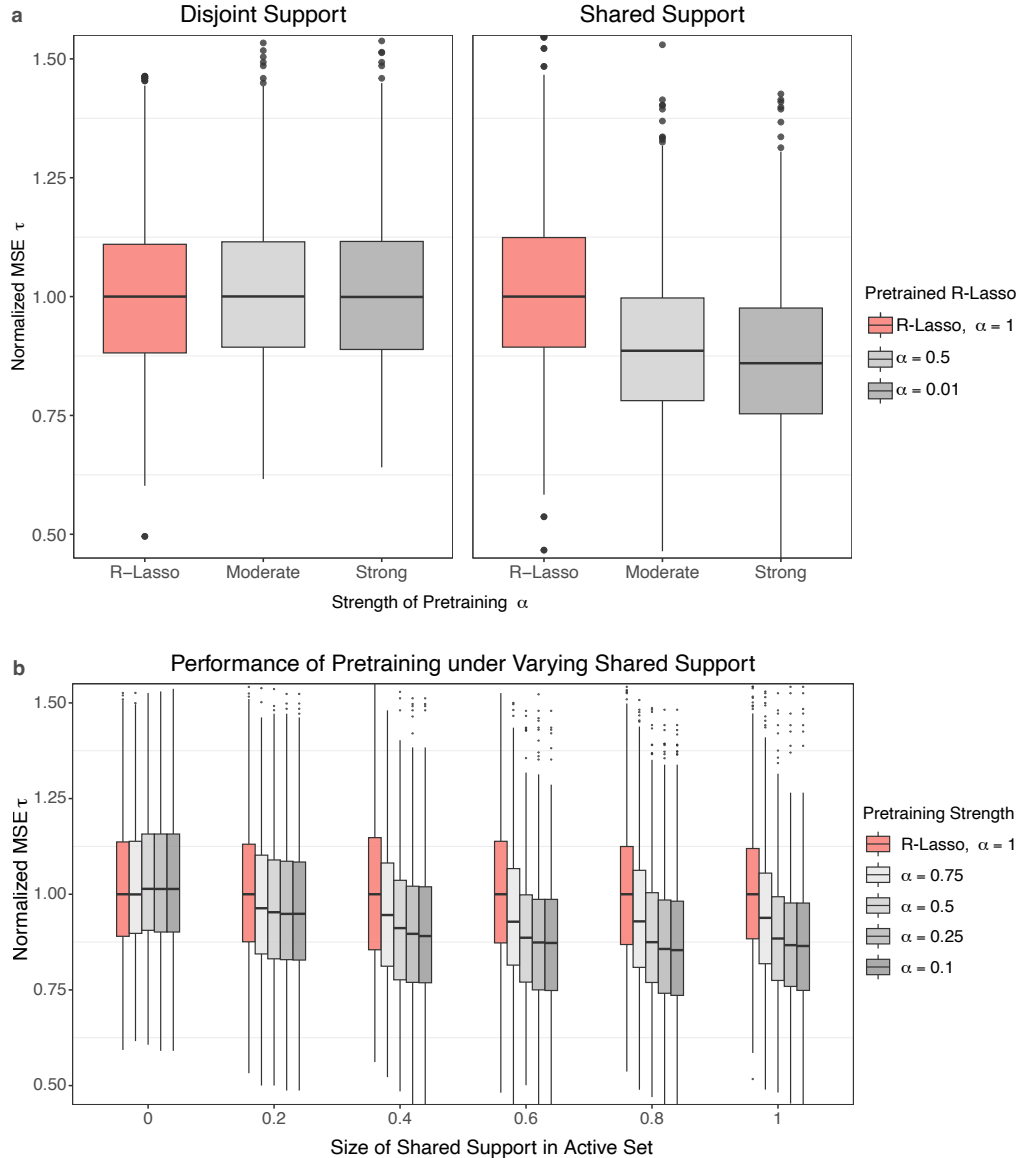


**Figure 3: Effect of Pretraining on CATE Estimation in terms of MSE.** The figure shows the performance of the R-lasso with (grey shades) and without pre-training (red) in a linear setting with  $n = 500$ ,  $p = 150$ , and  $SNR = 2$  and an active set of size  $|S| = \frac{p}{3}$ . Panel a shows the performance in two settings: with disjoint support between  $m(X_i)$  and  $\tau(X_i)$  (left) and shared support (right). The hyperparameter  $\alpha$  denotes different pretraining strengths, where  $\alpha = 1$  is equivalent to the R-lasso without pretraining and increasing pretraining strengths as  $\alpha$  approaches 0.

While the previous experiments showed a clear advantage for pretraining in settings

with overlap, it requires the correct selection of the pretraining strength  $w_j = \frac{1}{\alpha}$ . Since the true  $\tau(X_i)$  is not available to us, we need to rely on a surrogate loss and turn to the  $R$ -loss. Figure 4 shows the concordance between the  $R$ -loss estimated from the training set and the mean squared error (MSE) estimates on the test set. Encouragingly, the  $R$ -loss proves to be concordant with the MSE and allows us to pick  $\alpha$  at which the test error is minimized. As we vary the size of overlap between prognostic and predictive factors, the pretrained  $R$ -lasso favors a lower  $\alpha$  (stronger pretraining) as expected.

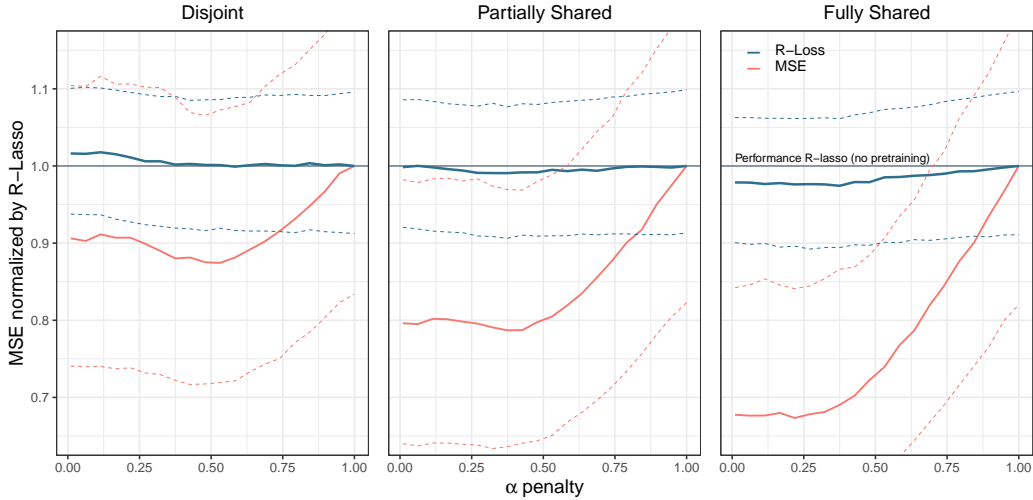


**Figure 4: Concordance of Training Set  $R$ -Loss and Test Set MSE.** The figure shows the median performance (standardized by the median  $R$ -lasso without pretraining) over different pretraining strengths of the  $R$ -lasso in a linear setting with  $n = 500$ ,  $p = 150$ ,  $SNR = 2$ , an active set of size  $|S| = \frac{p}{3}$  and for 5000 repetitions. The results are stratified by the size of shared support between prognostic and predictive factors: disjoint (left), partially shared (middle) and fully shared support (right panel). The minimum test set MSE and training set  $R$ -loss are concordant. In settings with stronger overlap, stronger pretraining (lower  $\alpha$ ) is favorable. The solid line at 1.0 shows the  $R$ -lasso without pretraining ( $\alpha = 1$ ) for comparison. Error bars denote the interquartile range between the 25th and 75th percentiles.

### 3.2 Assessing Power to Detect Heterogeneity

The end goal of fitting CATE models is to discover potential subgroups or strata as defined by our predictor variables  $X_i$  that have average treatment effects that differ meaningfully from the overall population average. Quantifying their ability to achieve this goal provides valuable information. Recently proposed metrics useful for this task take inspiration from predictive analysis tools such as the ROC curve

and include Chernozhukov et al. (2018), Radcliffe (2007), Sverdrup et al. (2024), Imai & Li (2023), Yadlowsky et al. (2025). An intuitive approach to operationalize this is to take inspiration from classical machine learning, where define a training set for fitting a CATE model, and evaluate its performance on a held-out test set. We can then rank individuals from highest to lowest predicted CATE. In the presence of heterogeneity, this should yield a decreasing quantile average treatment effect as we move from higher to lower quantiles. One way to operationalize this CATE-based ranking is to use the targeting operator characteristic (TOC) curve (Yadlowsky et al. 2025), defined as

$$\text{TOC}(q) = \mathbb{E} \left[ Y_i(1) - Y_i(0) \mid \hat{\tau}(X_i) \geq F_{\hat{\tau}(X_i)}^{-1}(1 - q) \right] - \mathbb{E} [Y_i(1) - Y_i(0)]. \quad (11)$$

The area under the TOC (AUTOC) is a numeric measure of heterogeneity and allows us to evaluate whether and how well our CATE model detects heterogeneity against a sharp null of no heterogeneity detected. One limitation of this approach is that train-test splits can be costly and suffer from random split sensitivity, especially in settings with small sample sizes. To overcome this limitation, we adopt a sequential cross-fold approach (Wager 2024).

Using the TOC curve, we can assess the power at which our CATE model detects heterogeneity. We hypothesized that in the presence of shared support, the pretrained  $R$ -lasso should be more powerful in detecting heterogeneity than without pretraining. For this experiment, we slightly tweak our DGP to a more challenging setting and reduce the support size to  $p/10$ , half of which is shared between  $m(X_i)$  and  $\tau(X_i)$  and the rest disjoint. We further introduce correlation among our covariates  $X \sim \mathcal{N}_p(\mathbf{0}, \Sigma)$ , where  $\Sigma$  is a Toeplitz matrix with entries  $\Sigma_{ij} = 0.5^{|i-j|}$  and reduce the SNR to 0.5. Figure 5 shows the TOC curve in two configurations: fully disjoint support and partially shared support. In the presence of overlap, the pretrained  $R$ -lasso shows a superior AUTOC as well as high power in detecting heterogeneity as we vary the the sample size  $n$  and the number of covariates  $p$  (Figure 6).

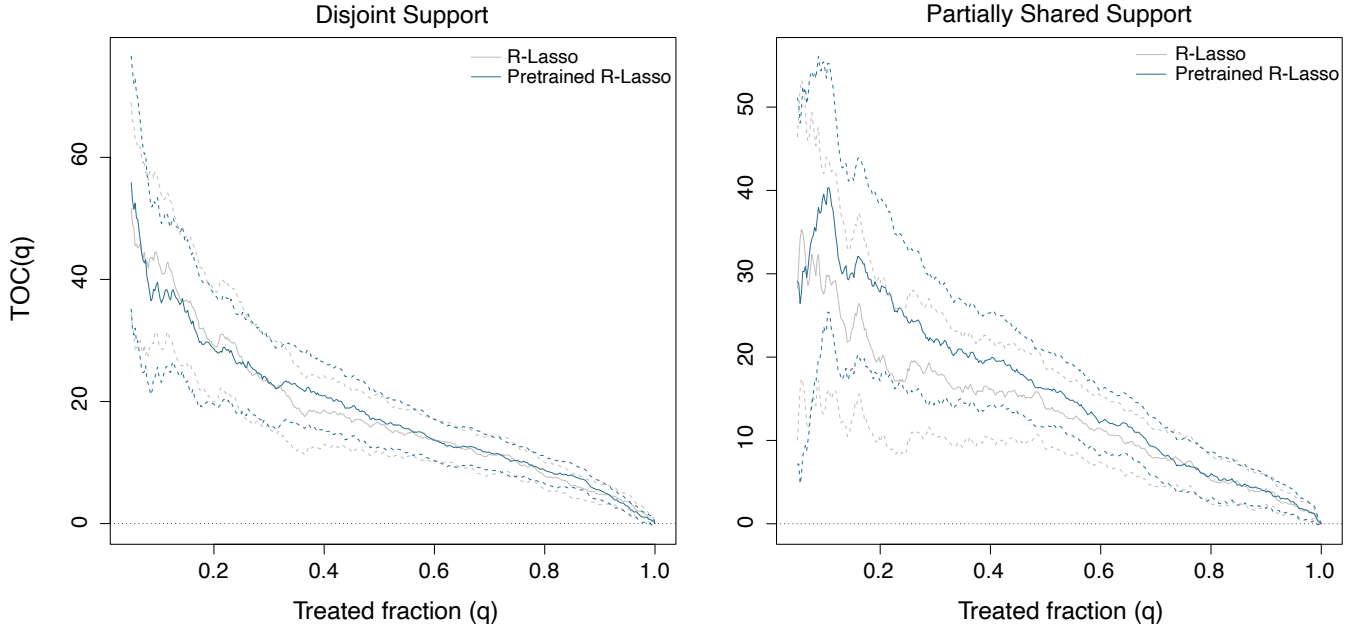


**Figure 5: TOC-based Comparison of R-lasso with and without Pretraining.** The figure shows the Targeting Operator Characteristic curves for the two R-lasso configurations and in settings with (blue) and without (gray) shared support. Dashed lines denote 95% confidence intervals based on the normal distribution. Earlier quintiles show higher average treatment effects. This experiment is conducted for a sparsity of  $\kappa = 0.1$ ,  $p = 500$ ,  $n = 1000$ ,  $SNR = 2$  and a shared support size of  $p \cdot \kappa \cdot 0.7$ .

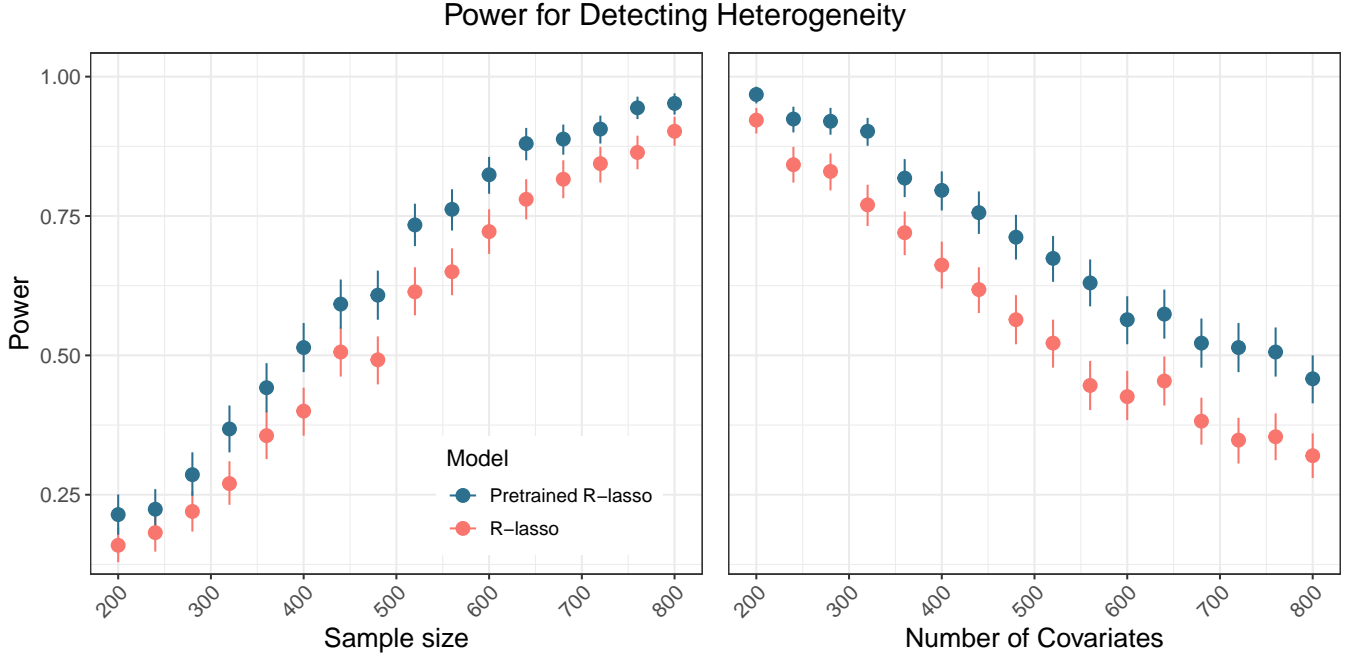


**Figure 6: Power in Detecting Heterogeneous Treatment Effects.** The figure shows the power of detecting heterogeneity for the pretrained and default R-lasso. The experiment is repeated 200 times under 5-fold sequential cross-validation and sparsity of  $\kappa = 0.1$ , joint support size of  $p \cdot \kappa \cdot 0.7$ ,  $SNR = 0.5$ , while varying  $n$  (left panel,  $p = 200$ ) or varying  $p$  (right panel,  $n = 800$ ). Error bars denote 95% bootstrapped confidence interval.

### 3.3 Sparsity and Reliable Support Recovery: uniR-Lasso

As demonstrated in the previous section, the effectiveness of our pretraining strategy depends both on the presence of overlap and the  $m(X_i)$  model’s ability to accurately detect it. The lasso has shown to be less reliable for this task in the presence of highly correlated futures and false positives in the active set (Su et al. 2017). To address this concern, Chatterjee et al. (2025) recently developed a univariate-guided sparse regression termed “UniLasso” that achieves higher sparsity by constraining the coefficients to have the same sign and reflecting their absolute magnitudes in univariate regression.

Sparsity is also a desirable property in our setting as it will result in more covariates being penalized. Specifically, it will result in stronger, more precise pretraining when fitting the model for  $\tau(X_i)$ . In addition, this model also achieves higher interpretability in high-dimensional settings with low signal, which might be desirable in many settings. As highlighted by Candes et al. (2018), identifying a subset of

relevant covariates, while controlling false discovery rates (FDR), is highly valuable in many areas ([Storey & Tibshirani 2003](#)). For example in biology, the reliable identification of a single driver of heterogeneity can help discover a larger regulatory network that modifies treatment effects.

Figure 7 shows the  $R$ -lasso and Uni $R$ -Lasso in a side-by-side comparison in terms of MSE, size of the active set, FDR and the Jaccard index for the DGP described in [subsection 3.2](#). The pretraining strength for both models is determined using the  $R$ -loss on the test data. The results show comparable performance in terms of MSE for both models. However, uni $R$ -lasso shows superior control of FDR and a better support recovery as measured by the Jaccard Index. Both models further benefit from pretraining proportionally to the size of shared support.

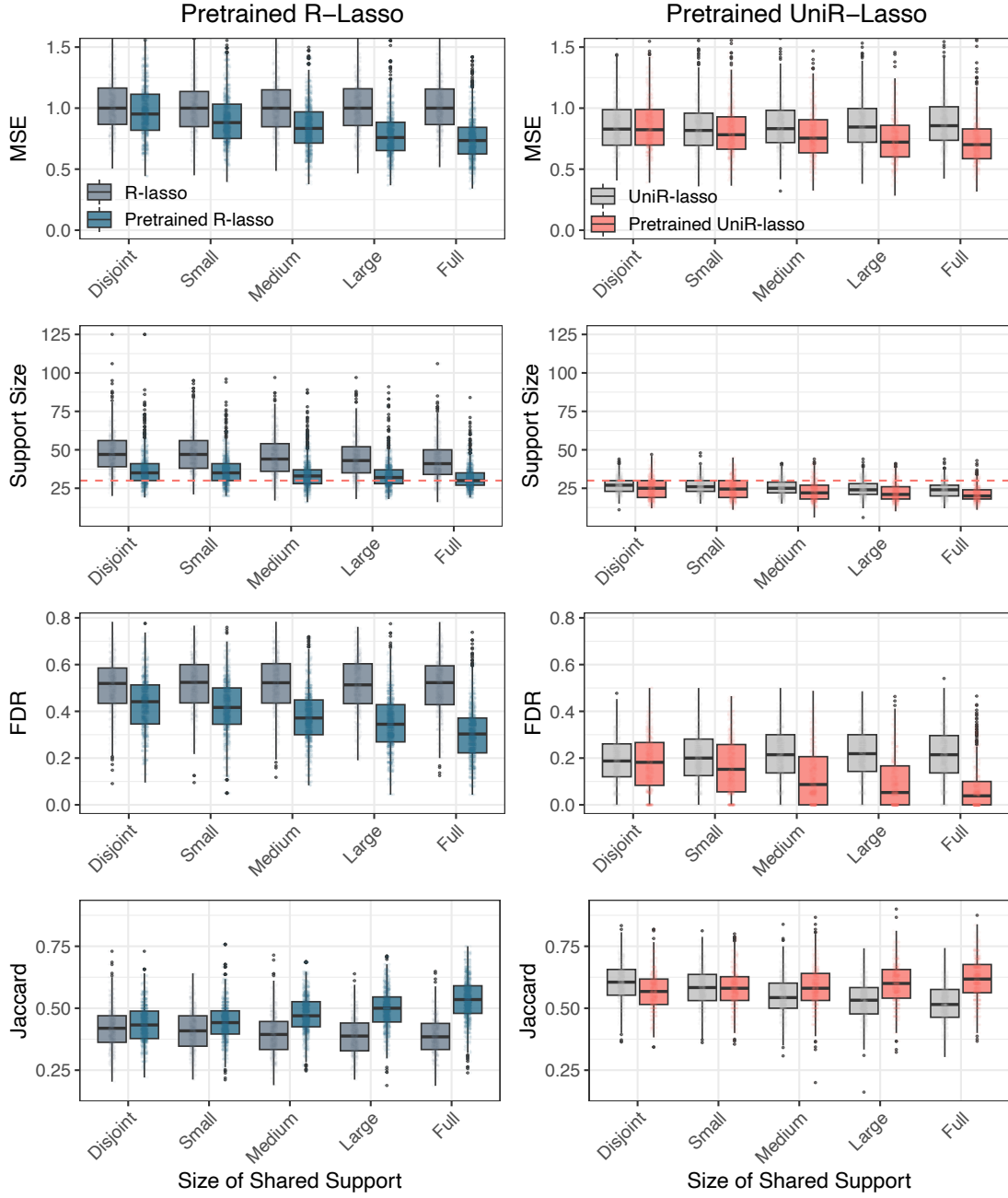


**Figure 7: Comparison of Pretraining for R-lasso and UniR-lasso** The figure shows the performance in terms of mean squared error (MSE), Support Size (red dashed indicates the true support), False Discovery Rate (FDR) and Jaccard Index. The MSE is normalized by the R-lasso for each shared support size setting. The experiment is conducted using the DGP described [subsection 3.2](#), with  $p = 300$ ,  $n = 500$  and  $SNR = 2$ . The strength of pretraining  $\alpha$  is determining using the R-loss for both learners.

## 4 Leveraging Side Information in Non-Linear Settings

In many applications, the mean outcome and CATE functions might involve complex interactions and non-linearities that the linear lasso outlined in [section 3](#) may not capture. A straightforward solution to continue using the lasso without modifying [Algorithm 1](#) is to substitute the feature matrix  $X_i$  with  $\psi(X_i)$  where  $\psi : \mathcal{X} \mapsto \mathbb{R}^d$  is some some featurization that maps the covariates to a richer  $d$ -dimensional space.  $\psi$  could, for example, be a collection of polynomial basis function. With a rich set of basis functions this approach can sufficiently capture complicated CATE or mean outcome functions (e.g., [Chen \(2007\)](#)). While a wide variety of basis expansions exist and the optimal choice is often application-specific ([Friedman 1991](#)), here we concentrate on gradient boosted trees to generate these basis expansions ([Chen & Guestrin 2016](#), [Friedman 2001](#)) and use the statistical software package `xgboost` ([Chen & Guestrin 2016](#)). Gradient boosting is an additive model that fits a sequence of weighted trees or weak learners. We explore its use in the  $R$ -learner for  $M = 100$  and  $500$  boosting rounds and a tree depth of  $1$  (stump). This results in a total of  $M$  trees (and thus new features), each of which performs a single split. As we increase the tree depth and number of boosting rounds, the transformed feature space is able to capture more complex relations, but also suffers from higher dimensions. To perform hyperparameter tuning, i.e. select the strength of pretraining and the number of boosting rounds, we use the  $R$ -loss. By concatenating this new feature matrix with our original one, the lasso can now pick from the original and transformed features. This is particularly useful in partially linear settings, where estimating  $m(X_i)$  and  $\tau(X_i)$  might require a model capable of handling both linear and non-linear components simultaneously. Depending on whether we expect  $m(X_i)$  and  $\tau(X_i)$  to differ substantially in their functional forms, we can generate distinct sets of basis functions tailored to each prediction task in the  $R$ -learner.

The lasso solution to sharing side-information leverages the lasso's adaptive regularization feature, but similar logic can be applied to other learners, such as random forests. Causal forests ([Athey et al. 2019](#)) are forest-based instantiations of the  $R$ -learner that uses regression forests for  $m(X_i)$  and  $e(X_i)$ , and then fits  $\tau(X_i)$  using a forest-weighted version of [\(3\)](#) designed to express heterogeneity in the CATE. As trees rely on split criteria rather than shrinking coefficients as in the lasso, we require a new strategy that allows us to leverage "side information". An effective way to improve random forests is to use adaptive feature-weighting (e.g., [Basu et al. \(2018\)](#)). Adapted to our setting, this procedure consists of fitting a random forest for  $m(X_i)$ , deriving the feature importance score for each covariate, and, finally, sampling each feature in  $\tau(X_i)$  with a probability that reflects its importance in  $m(X_i)$ . As for the lasso, we can introduce a hyperparameter that determines the strength at which the feature importance gets translated into differential feature sampling. We refer to this approach as "Pretrained GRF". A related approach is to use  $m(X_i)$  for select-

ing/discard features based on their importance. If a given feature’s importance is below a certain threshold in grf (“prescreened GRF”) it is dropped or sampled with higher probability based on its coefficients from a lasso model (“lasso-prescreened GRF”), when estimating the  $\tau(X_i)$  model. Figure 8 shows the performance of these modified CATE estimators using the DGP described in subsection 3.2 using the grf package (Tibshirani et al. 2024).

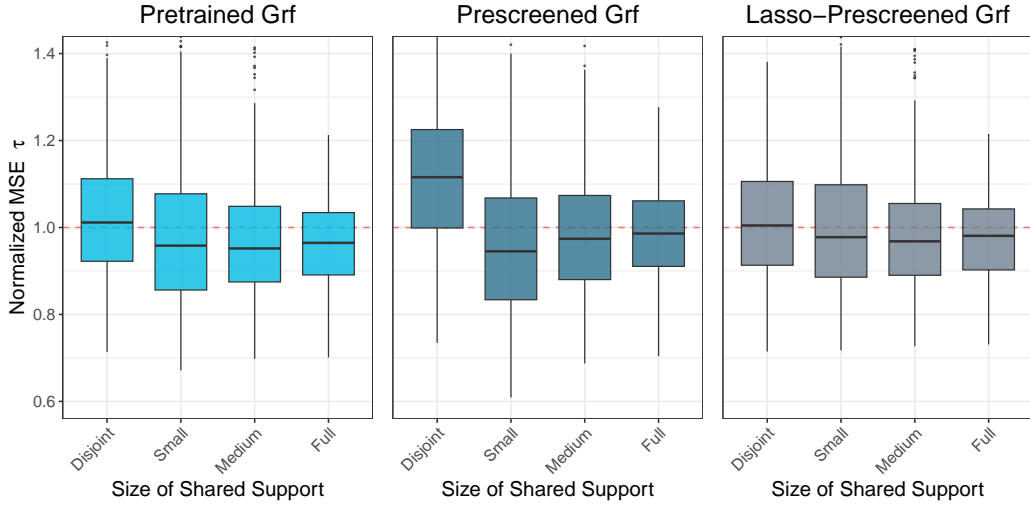


**Figure 8: Effect of Pretraining Strategies for Generalized Random Forests (GRF).** The figure shows the performance in terms of mean squared error (MSE), normalized by the baseline GRF, in three different configurations: when using weighted feature sampling based on  $m(x)$  (“Pretrained GRF”, left panel), prior variable prescreening and removal (“Prescreened GRF”, middle pane) based on importance scores, and prescreening based on the lasso (“Lasso-Prescreened GRF”, right panel). The experiment is conducted using the DGP described in subsection 3.2, with  $p = 150$ ,  $n = 500$  and  $SNR = 2$ . The degree at which importance scores from  $m(x)$  are translated into differential feature sampling/screening is determined by the  $R$ -loss.

Finally, we test these models against the pretrained  $R$ -lasso in combination with basis expansions generated by a gradient boosted tree. To test these approaches we modified four DGPs developed by Nie & Wager (2021). We consider four setups A-D, each varying in the complexity of the treatment effect  $\tau(X_i)$  and the main effects function  $\mu_{(0)}(X_i)$ . Setups A-C assume a randomized controlled trial with  $e(X_i) = 0.5$ , while the propensities in D are given by  $e(X_i) = 1/(1 + \exp(-X_{i1}) + \exp(-X_{i2}))$ . Covariates are generated as  $X \sim \mathcal{N}(0, 1)^{n \times p}$ . Setup A features a non-linear baseline main effect given by  $\mu_{(0)}(X_i) = \sin(\cdot X_{i1} X_{i2}) + 2(X_{i3} - 0.5)^2 + X_{i4}^3 + 0.5X_{i5}^3$  and a linear treatment effect, defined as  $\tau(X_i) = (\sum_{j=1}^5 X_{ij})/5$ . Setup

B introduces high-dimensional interactions:  $\mu_{(0)}(X_i) = \max\{0, X_{i1}^2 + X_{i2}^2, X_{i3}^2\} + \max\{0, X_{i4}^2 + X_{i5}^2\} + X_{i6}^2 + X_{i7}^2$  and a more complex, non-linear treatment effect:  $\tau(X_i) = X_{i1}^2 + \log(1 + \sum_{j=2}^5 e^{X_{ij}})$ . Setup C flips the structure of setup A: the baseline function is linear and the treatment effect is complex. The outcome model is  $\mu_{(0)}(X_i) = (\sum_{j=1}^5 X_{ij})/5 + 0.8(X_{i6} + X_{i7})$  and the treatment effect is defined as  $\tau(X_i) = \max\{0, \sum_{j=1}^3 X_{ij} + \max\{0, X_{i4}^2 + X_{i5}^2\} + X_{i6}^2 + X_{i7}^2 + 0.5(X_{i8} + X_{i9})\}$ . Finally, Setup D presents a baseline outcome that combines piecewise linearity and quadratic effects:  $\mu_{(0)}(X_i) = [\max\{0, \sum_{j=1}^3 X_{ij}\} + \max\{0, X_{i4} + X_{i5}\}]/2 + X_{i6}^2 + X_{i7}^2$ . The treatment effect is composed of contrasting additive and subtractive components:  $\tau(X_i) = \max\{0, \sum_{j=1}^3 X_{ij}\} - \max\{0, X_{i4} + X_{i5}\} + X_{i9}^2 + X_{i10}^2$ .

Figure 9 shows the performance of all models including the (pretrained)  $R$ -lasso, (pretrained) GRF, and  $R$ -Boost. We further include two  $R$ -lasso models (with and without pretraining) that take basis expansions generated from xgboost, concatenated with the original design matrix, as input: the first model configuration uses the basis functions generated from the fit on  $m(X_i)$ ; the second leverages basis functions generated from fits on both  $m(X_i)$  and  $\tau(X_i)$ , but shields the basis functions generated from the latter from any pretraining penalties. We report results for all combinations of  $n \in \{500, 1000\}$ ,  $p \in \{15, 30\}$  and  $\text{SNR} \in \{0.5, 2\}$ .

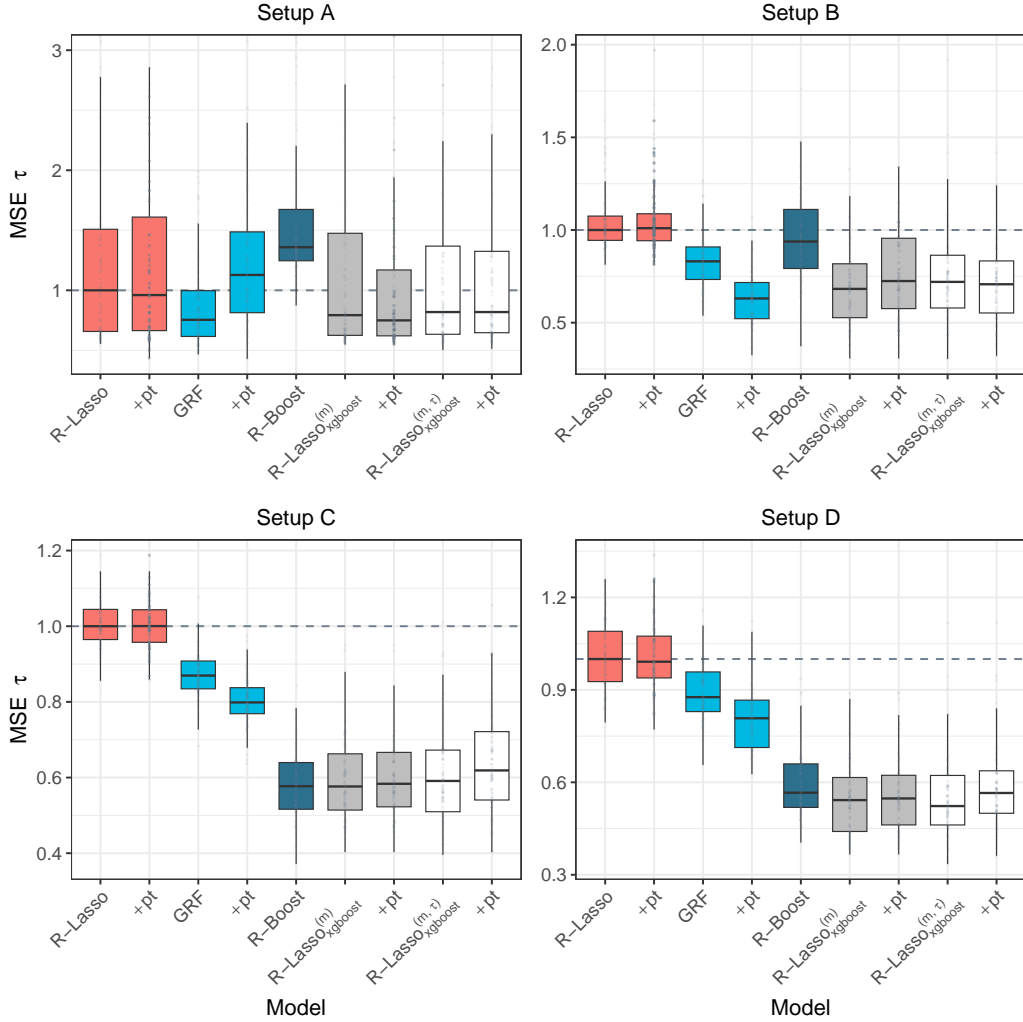


**Figure 9: Comparison of CATE Estimators in Non-linear Settings.** The figure shows the performance in terms of mean squared error (MSE), normalized by the baseline R-lasso. The experiment is conducted using the DGPs described for setups A-D, with  $p = 30$ ,  $n = 1000$  and  $SNR = 2$ . The degree of pretraining in each model is determined by the R-loss. The R-lasso models with subscripts  $xgboost$  denote models that take basis functions generated from the fit on of an xgboost on  $m(X_i)$  as input. The model with superscript  $(m, \tau)$  leverages basis functions generated from both fits on  $m(X_i)$  and  $\tau(X_i)$ . The dashed line indicates the performance of the R-lasso by which all MSEs are standardized.

## 5 Discussion

In this paper we present a new approach to pretrain CATE models that minimize a causal loss function. Our pretraining strategy is motivated by a real-world phenomenon that give rise to distinct structural patterns in the data. In many settings, factors associated with prognosis are also predictive of high treatment effects. The intuition behind our approach is that rather than treating the estimates from the mean outcome model and the propensity model as mere nuisance parameters, we leverage their supports as “side information”. This allows us to improve on our CATE estimation and synergize independent prediction tasks in the *R*-learner. While our exposition focused mostly on the lasso, we also demonstrated how our pretraining approach can be extended to settings with multicollinearity using the uni*R*-lasso or to non-linear settings via basis functions and generalized random forests. Employing this pretraining strategy in the *R*-learner resulted in lower error rates, higher power in detecting heterogeneity, and lower false discovery rates, which is particularly relevant in fields like biomarker discovery.

One limitation of our pretraining approach is that it offers no performance benefit in scenarios with minimal or no overlap between predictive and prognostic factors. In such settings, it is possible that pretraining might lead to over-regularization of the wrong covariates and prioritize strong predictors in the shared support over disjoint weak predictors in the treatment effect function. This property might not be favorable, especially when treatment effects are spread out across a few strong and many weak predictors. Another limitation is the dependence on the *R*-loss for correct choice of  $\alpha$  and other hyperparameters: if the estimation error for nuisance parameters is large, the *R*-loss becomes less reliable for such hyperparameters.

A number of important extensions of our approach are left option. The proposed forms of supervised pretraining used in this work is demonstrated for settings where researchers have access to a single dataset. However, in many settings it might be valuable to pretrain CATE models on an additional external dataset. Our approach can be simply extented to those setting as it is possible to pretrain the models for  $m(X_i)$ ,  $e(X_i)$  and  $\tau(X_i)$  using an external dataset. [Craig et al. \(2024\)](#) demonstrate that training a predictive model across multiple tumor types and then transferring knowledge from this pan-cancer model to a subtype-specific model (e.g., for breast cancer) can lead to improved predictive accuracy. Similarly, in cancer trials that are further stratified by biomarkers, it might be beneficial to pretrain a model on the total trial population (intention-to-treat) and transfer this information into a CATE model fit on a subgroup that is enriched for a given biomarker. This can help overcome some settings with limited sample size, high dimensions, and low signal.

In follow-up work, we aim to demonstrate the utility of this approach in real-world data from clinical settings, with a focus on applications in oncology.

## Acknowledgments

We are grateful to Erin Craig, Trevor Hastie, Guido Imbens, Ying Lu, Jonathan Taylor, Lu Tian and Stefan Wager as well as seminar participants at Stanford University for valuable comments and feedback.

R.T. was supported by the NIH (5R01EB001988-16) and the NSF (19DMS1208164).

## References

Alizadeh, A. A., Eisen, M. B., Davis, R. E., Ma, C., Lossos, I. S., Rosenwald, A., Boldrick, J. C., Sabet, H., Tran, T., Yu, X. et al. (2000), ‘Distinct types of diffuse large b-cell lymphoma identified by gene expression profiling’, *Nature* **403**(6769), 503–511.

Argyriou, A., Evgeniou, T. & Pontil, M. (2006), ‘Multi-task feature learning’, *Advances in neural information processing systems* **19**.

Athey, S. & Imbens, G. (2016), ‘Recursive partitioning for heterogeneous causal effects’, *Proceedings of the National Academy of Sciences* **113**(27), 7353–7360.

Athey, S., Keleher, N. & Spiess, J. (2025), ‘Machine learning who to nudge: causal vs predictive targeting in a field experiment on student financial aid renewal’, *Journal of Econometrics* p. 105945.

Athey, S., Tibshirani, J. & Wager, S. (2019), ‘Generalized random forests’, *The Annals of Statistics* **47**(2), 1148–1178.

Ballman, K. V. (2015), ‘Biomarker: predictive or prognostic?’, *Journal of clinical oncology: official journal of the American Society of Clinical Oncology* **33**(33), 3968–3971.

Basu, S., Kumbier, K., Brown, J. B. & Yu, B. (2018), ‘Iterative random forests to discover predictive and stable high-order interactions’, *Proceedings of the National Academy of Sciences* **115**(8), 1943–1948.

Candes, E., Fan, Y., Janson, L. & Lv, J. (2018), ‘Panning for gold:‘model-x’knockoffs for high dimensional controlled variable selection’, *Journal of the Royal Statistical Society Series B: Statistical Methodology* **80**(3), 551–577.

Carney, R. M. & Freedland, K. E. (2017), ‘Depression and coronary heart disease’, *Nature Reviews Cardiology* **14**(3), 145–155.

Chapuy, B., Stewart, C., Dunford, A. J., Kim, J., Kamburov, A., Redd, R. A., Lawrence, M. S., Roemer, M. G., Li, A. J., Ziepert, M. et al. (2018), ‘Molecular

subtypes of diffuse large b cell lymphoma are associated with distinct pathogenic mechanisms and outcomes', *Nature medicine* **24**(5), 679–690.

Chatterjee, S., Hastie, T. & Tibshirani, R. (2025), 'Univariate-guided sparse regression', *arXiv preprint arXiv:2501.18360* .

Chen, T. & Guestrin, C. (2016), Xgboost: A scalable tree boosting system, *in* 'Proceedings of the 22nd acm sigkdd international conference on knowledge discovery and data mining', pp. 785–794.

Chen, X. (2007), 'Large sample sieve estimation of semi-nonparametric models', *Handbook of econometrics* **6**, 5549–5632.

Chernozhukov, V., Demirer, M., Duflo, E. & Fernandez-Val, I. (2018), Generic machine learning inference on heterogeneous treatment effects in randomized experiments, with an application to immunization in india, Technical report, National Bureau of Economic Research.

Cohen, Z. D. & DeRubeis, R. J. (2018), 'Treatment selection in depression', *Annual review of clinical psychology* **14**(1), 209–236.

Craig, E., Pilanci, M., Menestrel, T. L., Narasimhan, B., Rivas, M., Dehghannasiri, R., Salzman, J., Taylor, J. & Tibshirani, R. (2024), 'Pretraining and the lasso', *arXiv preprint arXiv:2401.12911* .

DiMatteo, M. R., Lepper, H. S. & Croghan, T. W. (2000), 'Depression is a risk factor for noncompliance with medical treatment: meta-analysis of the effects of anxiety and depression on patient adherence', *Archives of internal medicine* **160**(14), 2101–2107.

Dobriban, E., Fortney, K., Kim, S. K. & Owen, A. B. (2015), 'Optimal multiple testing under a gaussian prior on the effect sizes', *Biometrika* **102**(4), 753–766.

Earle, C. C., Landrum, M. B., Souza, J. M., Neville, B. A., Weeks, J. C. & Ayanian, J. Z. (2008), 'Aggressiveness of cancer care near the end of life: is it a quality-of-care issue?', *Journal of clinical oncology* **26**(23), 3860–3866.

Fortney, K., Dobriban, E., Garagnani, P., Pirazzini, C., Monti, D., Mari, D., Atzman, G., Barzilai, N., Franceschi, C., Owen, A. B. et al. (2015), 'Genome-wide scan informed by age-related disease identifies loci for exceptional human longevity', *PLoS genetics* **11**(12), e1005728.

Foster, D. J. & Syrgkanis, V. (2023), 'Orthogonal statistical learning', *The Annals of Statistics* **51**(3), 879–908.

Friedman, J. H. (1991), 'Multivariate adaptive regression splines', *The annals of statistics* **19**(1), 1–67.

Friedman, J. H. (2001), ‘Greedy function approximation: a gradient boosting machine’, *Annals of statistics* pp. 1189–1232.

Friedman, J. H., Hastie, T. & Tibshirani, R. (2010), ‘Regularization paths for generalized linear models via coordinate descent’, *Journal of statistical software* **33**, 1–22.

Gu, T., Han, Y. & Duan, R. (2024), ‘Robust angle-based transfer learning in high dimensions’, *Journal of the Royal Statistical Society Series B: Statistical Methodology* .

Hastie, T., Tibshirani, R., Friedman, J. H. & Friedman, J. H. (2009), *The elements of statistical learning: data mining, inference, and prediction*, Vol. 2, Springer.

Hudis, C. A. (2007), ‘Trastuzumab—mechanism of action and use in clinical practice’, *New England journal of medicine* **357**(1), 39–51.

Ignatiadis, N. & Huber, W. (2021), ‘Covariate powered cross-weighted multiple testing’, *Journal of the Royal Statistical Society Series B: Statistical Methodology* **83**(4), 720–751.

Imai, K. & Li, M. L. (2023), ‘Experimental evaluation of individualized treatment rules’, *Journal of the American Statistical Association* **118**(541), 242–256.

Imai, K. & Ratkovic, M. (2013), ‘Estimating treatment effect heterogeneity in randomized program evaluation’, *The Annals of Applied Statistics* **7**(1).

Imbens, G. W. & Rubin, D. B. (2015), *Causal inference in statistics, social, and biomedical sciences*, Cambridge university press.

Kennedy, E. H. (2023), ‘Towards optimal doubly robust estimation of heterogeneous causal effects’, *Electronic Journal of Statistics* **17**(2), 3008–3049.

Kennedy, E. H., Balakrishnan, S., Robins, J. M. & Wasserman, L. (2024), ‘Minimax rates for heterogeneous causal effect estimation’, *The Annals of Statistics* **52**(2), 793–816.

Kent, D. M., Nelson, J., Dahabreh, I. J., Rothwell, P. M., Altman, D. G. & Hayward, R. A. (2016), ‘Risk and treatment effect heterogeneity: re-analysis of individual participant data from 32 large clinical trials’, *International journal of epidemiology* **45**(6), 2075–2088.

Kent, D. M., Paulus, J. K., Van Klaveren, D., D’Agostino, R., Goodman, S., Hayward, R., Ioannidis, J. P., Patrick-Lake, B., Morton, S., Pencina, M. et al. (2020), ‘The predictive approaches to treatment effect heterogeneity (path) statement’, *Annals of internal medicine* **172**(1), 35–45.

Kosorok, M. R. & Laber, E. B. (2019), 'Precision medicine', *Annual review of statistics and its application* **6**(1), 263–286.

Kravitz, R. L., Duan, N. & Braslow, J. (2004), 'Evidence-based medicine, heterogeneity of treatment effects, and the trouble with averages', *The Milbank Quarterly* **82**(4), 661–687.

Künzel, S. R., Sekhon, J. S., Bickel, P. J. & Yu, B. (2019), 'Metalearners for estimating heterogeneous treatment effects using machine learning', *Proceedings of the national academy of sciences* **116**(10), 4156–4165.

Li, S., Cai, T. T. & Li, H. (2022), 'Transfer learning for high-dimensional linear regression: Prediction, estimation and minimax optimality', *Journal of the Royal Statistical Society Series B: Statistical Methodology* **84**(1), 149–173.

Lichtman, J. H., Froelicher, E. S., Blumenthal, J. A., Carney, R. M., Doering, L. V., Frasure-Smith, N., Freedland, K. E., Jaffe, A. S., Leifheit-Limson, E. C., Sheps, D. S. et al. (2014), 'Depression as a risk factor for poor prognosis among patients with acute coronary syndrome: systematic review and recommendations: a scientific statement from the american heart association', *Circulation* **129**(12), 1350–1369.

Manski, C. F. (2004), 'Statistical treatment rules for heterogeneous populations', *Econometrica* **72**(4), 1221–1246.

Modi, S., Jacot, W., Yamashita, T., Sohn, J., Vidal, M., Tokunaga, E., Tsurutani, J., Ueno, N. T., Prat, A., Chae, Y. S. et al. (2022), 'Trastuzumab deruxtecan in previously treated her2-low advanced breast cancer', *New England Journal of Medicine* **387**(1), 9–20.

Morzywolek, P., Decruyenaere, J. & Vansteelandt, S. (2023), 'On a general class of orthogonal learners for the estimation of heterogeneous treatment effects', *arXiv preprint arXiv:2303.12687*.

National Cancer Institute (2025a), 'Predictive factor', NCI Dictionary of Cancer Terms. Accessed: 2025-01-05.  
**URL:** <https://www.cancer.gov/publications/dictionaries/cancer-terms/def/predictive-factor>

National Cancer Institute (2025b), 'Prognostic factor', NCI Dictionary of Cancer Terms. Accessed: 2025-01-05.  
**URL:** <https://www.cancer.gov/publications/dictionaries/cancer-terms/def/prognostic-factor>

Nie, X. & Wager, S. (2021), 'Quasi-oracle estimation of heterogeneous treatment effects', *Biometrika* **108**(2), 299–319.

Obozinski, G., Taskar, B. & Jordan, M. I. (2010), 'Joint covariate selection and joint subspace selection for multiple classification problems', *Statistics and Computing* **20**, 231–252.

Powers, S., Qian, J., Jung, K., Schuler, A., Shah, N. H., Hastie, T. & Tibshirani, R. (2018), 'Some methods for heterogeneous treatment effect estimation in high dimensions', *Statistics in medicine* **37**(11), 1767–1787.

R Core Team (2024), 'R: A language and environment for statistical computing'. <https://www.R-project.org/>.

Radcliffe, N. (2007), 'Using control groups to target on predicted lift: Building and assessing uplift model', *Direct Marketing Analytics Journal* pp. 14–21.

Ribas, A., Puzanov, I., Dummer, R., Schadendorf, D., Hamid, O., Robert, C., Hodi, F. S., Schachter, J., Pavlick, A. C., Lewis, K. D. et al. (2015), 'Pembrolizumab versus investigator-choice chemotherapy for ipilimumab-refractory melanoma (keynote-002): a randomised, controlled, phase 2 trial', *The lancet oncology* **16**(8), 908–918.

Robins, J. M. (2004), Optimal structural nested models for optimal sequential decisions, in 'Proceedings of the Second Seattle Symposium in Biostatistics: analysis of correlated data', Springer, pp. 189–326.

Robins, J. M., Rotnitzky, A. & Zhao, L. P. (1994), 'Estimation of regression coefficients when some regressors are not always observed', *Journal of the American statistical Association* **89**(427), 846–866.

Robinson, P. M. (1988), 'Root-n-consistent semiparametric regression', *Econometrica: Journal of the Econometric Society* pp. 931–954.

Rueda, O. M., Sammut, S.-J., Seoane, J. A., Chin, S.-F., Caswell-Jin, J. L., Callari, M., Batra, R., Pereira, B., Bruna, A., Ali, H. R. et al. (2019), 'Dynamics of breast-cancer relapse reveal late-recurring er-positive genomic subgroups', *Nature* **567**(7748), 399–404.

Shalit, U., Johansson, F. D. & Sontag, D. (2017), Estimating individual treatment effect: generalization bounds and algorithms, in 'International conference on machine learning', PMLR, pp. 3076–3085.

Slamon, D. J., Clark, G. M., Wong, S. G., Levin, W. J., Ullrich, A. & McGuire, W. L. (1987), 'Human breast cancer: correlation of relapse and survival with amplification of the her-2/neu oncogene', *science* **235**(4785), 177–182.

Slamon, D. J., Leyland-Jones, B., Shak, S., Fuchs, H., Paton, V., Bajamonde, A., Fleming, T., Eiermann, W., Wolter, J., Pegram, M. et al. (2001), 'Use of

chemotherapy plus a monoclonal antibody against her2 for metastatic breast cancer that overexpresses her2', *New England journal of medicine* **344**(11), 783–792.

Storey, J. D. & Tibshirani, R. (2003), 'Statistical significance for genomewide studies', *Proceedings of the National Academy of Sciences* **100**(16), 9440–9445.

Su, W., Bogdan, M. & Candes, E. (2017), 'False discoveries occur early on the lasso path', *The Annals of statistics* pp. 2133–2150.

Sverdrup, E., Wu, H., Athey, S. & Wager, S. (2024), 'Qini curves for multi-armed treatment rules', *Journal of Computational and Graphical Statistics* (just-accepted), 1–24.

Tibshirani, J., Athey, S., Friedberg, R., Hadad, V., Hirshberg, D., Miner, L., Sverdrup, E., Wager, S. & Wright, M. (2024), 'grf: Generalized random forests'. R package version 2.4.0. <https://github.com/grf-labs/grf>.

Tomasik, B., Garbicz, F., Braun, M., Bieńkowski, M. & Jassem, J. (2024), 'Heterogeneity in precision oncology', *Cambridge Prisms: Precision Medicine* **2**, e2.

van der Laan, L., Carone, M. & Luedtke, A. (2024), 'Combining T-learning and DR-learning: a framework for oracle-efficient estimation of causal contrasts', *arXiv preprint arXiv:2402.01972* .

Wager, S. (2024), 'Sequential validation of treatment heterogeneity', *arXiv preprint arXiv:2405.05534* .

Wager, S. & Athey, S. (2018), 'Estimation and inference of heterogeneous treatment effects using random forests', *Journal of the American Statistical Association* **113**(523), 1228–1242.

Weeks, J. C., Cook, E. F., O'Day, S. J., Peterson, L. M., Wenger, N., Reding, D., Harrell, F. E., Kussin, P., Dawson, N. V., Connors Jr, A. F. et al. (1998), 'Relationship between cancer patients' predictions of prognosis and their treatment preferences', *Jama* **279**(21), 1709–1714.

Yadlowsky, S., Fleming, S., Shah, N., Brunskill, E. & Wager, S. (2025), 'Evaluating treatment prioritization rules via rank-weighted average treatment effects', *Journal of the American Statistical Association* **120**(549).

Yeager, D. S., Hanselman, P., Walton, G. M., Murray, J. S., Crosnoe, R., Muller, C., Tipton, E., Schneider, B., Hulleman, C. S., Hinojosa, C. P. et al. (2019), 'A national experiment reveals where a growth mindset improves achievement', *Nature* **573**(7774), 364–369.

Yeager, D. S., Romero, C., Paunesku, D., Hulleman, C. S., Schneider, B., Hinojosa, C., Lee, H. Y., O'Brien, J., Flint, K., Roberts, A. et al. (2016), 'Using design thinking to improve psychological interventions: The case of the growth mindset during the transition to high school.', *Journal of educational psychology* **108**(3), 374.

Zou, H. (2006), 'The adaptive lasso and its oracle properties', *Journal of the American statistical association* **101**(476), 1418–1429.

## A Supplement

Table 1: Comparison of R-lasso and UniR-lasso (with Pretraining) in Linear Setting with Sparsity  $k = 0.1$

n	p	SNR	R-lasso		UniR-lasso	
			Base	+pt	Base	+pt
<i>Mean Squared Error</i>						
300	50	0.5	17.48 (17.12, 17.82)	14.33 (14.16, 14.48)	13.48 (13.18, 13.78)	<b>12.31 (12.04, 12.59)</b>
300	50	2.0	5.32 (5.22, 5.42)	4.08 (4.03, 4.13)	3.29 (3.21, 3.37)	<b>2.97 (2.89, 3.03)</b>
300	300	0.5	317.54 (314.58, 320.70)	295.88 (294.26, 297.67)	309.32 (306.55, 312.09)	<b>291.98 (289.58, 294.20)</b>
300	300	2.0	166.93 (165.21, 168.88)	<b>142.01 (141.14, 142.83)</b>	156.55 (154.97, 158.17)	144.85 (143.56, 146.22)
500	50	0.5	10.76 (10.57, 10.97)	8.50 (8.41, 8.59)	7.79 (7.63, 7.98)	<b>6.93 (6.78, 7.08)</b>
500	50	2.0	3.03 (2.96, 3.09)	2.27 (2.24, 2.30)	1.70 (1.66, 1.75)	<b>1.57 (1.53, 1.61)</b>
500	300	0.5	239.49 (236.99, 241.86)	<b>211.28 (209.95, 212.61)</b>	233.15 (230.81, 235.58)	217.83 (215.66, 220.02)
500	300	2.0	103.96 (102.97, 104.96)	86.05 (85.56, 86.57)	88.20 (87.20, 89.18)	<b>79.63 (78.76, 80.48)</b>
<i>Jaccard Index</i>						
300	50	0.5	0.41 (0.40, 0.42)	0.52 (0.51, 0.52)	0.56 (0.55, 0.56)	<b>0.58 (0.58, 0.59)</b>
300	50	2.0	0.50 (0.49, 0.50)	0.65 (0.64, 0.65)	0.83 (0.82, 0.83)	<b>0.87 (0.87, 0.88)</b>
300	300	0.5	0.13 (0.13, 0.13)	<b>0.16 (0.16, 0.16)</b>	0.13 (0.13, 0.13)	0.13 (0.13, 0.14)
300	300	2.0	0.32 (0.32, 0.32)	0.38 (0.38, 0.38)	0.38 (0.38, 0.38)	<b>0.40 (0.40, 0.40)</b>
500	50	0.5	0.47 (0.46, 0.48)	0.61 (0.60, 0.61)	0.70 (0.69, 0.71)	<b>0.74 (0.73, 0.75)</b>
500	50	2.0	0.50 (0.49, 0.51)	0.66 (0.66, 0.67)	0.86 (0.85, 0.86)	<b>0.89 (0.89, 0.90)</b>
500	300	0.5	0.23 (0.22, 0.23)	<b>0.28 (0.27, 0.28)</b>	0.24 (0.23, 0.24)	0.26 (0.25, 0.26)
500	300	2.0	0.40 (0.40, 0.40)	0.48 (0.48, 0.48)	0.56 (0.55, 0.56)	<b>0.59 (0.59, 0.59)</b>
<i>False Discovery Rate</i>						
300	50	0.5	0.47 (0.46, 0.48)	0.33 (0.32, 0.33)	0.19 (0.18, 0.19)	<b>0.14 (0.13, 0.14)</b>
300	50	2.0	0.49 (0.49, 0.50)	0.34 (0.33, 0.34)	0.15 (0.14, 0.15)	<b>0.10 (0.10, 0.11)</b>
300	300	0.5	0.44 (0.43, 0.46)	0.36 (0.35, 0.36)	0.39 (0.38, 0.40)	<b>0.18 (0.18, 0.19)</b>
300	300	2.0	0.52 (0.52, 0.53)	0.40 (0.39, 0.40)	0.27 (0.26, 0.27)	<b>0.14 (0.13, 0.14)</b>
500	50	0.5	0.48 (0.47, 0.49)	0.32 (0.32, 0.33)	0.16 (0.16, 0.17)	<b>0.11 (0.11, 0.12)</b>
500	50	2.0	0.50 (0.49, 0.51)	0.33 (0.33, 0.34)	0.14 (0.13, 0.15)	<b>0.10 (0.10, 0.11)</b>
500	300	0.5	0.49 (0.48, 0.50)	0.37 (0.37, 0.38)	0.32 (0.32, 0.33)	<b>0.18 (0.18, 0.19)</b>
500	300	2.0	0.51 (0.51, 0.52)	0.37 (0.37, 0.38)	0.21 (0.21, 0.21)	<b>0.13 (0.12, 0.13)</b>
<i>Support Size</i>						
300	50	0.5	8.94 (8.73, 9.15)	6.41 (6.32, 6.49)	4.40 (4.33, 4.48)	<b>4.18 (4.11, 4.26)</b>
300	50	2.0	11.47 (11.28, 11.67)	8.29 (8.21, 8.36)	5.96 (5.89, 6.02)	<b>5.64 (5.58, 5.69)</b>
300	300	0.5	15.79 (15.18, 16.36)	12.10 (11.87, 12.35)	8.70 (8.46, 8.93)	<b>6.57 (6.38, 6.79)</b>
300	300	2.0	36.82 (36.22, 37.42)	27.67 (27.43, 27.89)	19.21 (18.98, 19.47)	<b>16.02 (15.83, 16.21)</b>
500	50	0.5	10.16 (9.98, 10.37)	7.34 (7.27, 7.42)	5.22 (5.15, 5.29)	<b>4.93 (4.87, 4.99)</b>
500	50	2.0	11.72 (11.52, 11.92)	8.41 (8.33, 8.48)	6.05 (5.99, 6.10)	<b>5.78 (5.72, 5.83)</b>
500	300	0.5	25.17 (24.59, 25.73)	19.40 (19.15, 19.65)	13.18 (12.92, 13.44)	<b>12.13 (11.84, 12.42)</b>
500	300	2.0	46.11 (45.58, 46.66)	34.16 (33.94, 34.40)	25.66 (25.45, 25.86)	<b>23.42 (23.16, 23.67)</b>

**Table 2: Comparison of CATE Estimators in Non-linear Settings: Test Set MSE**

Setup	n	p	SNR	R-lasso					R-boost		GRF	
				Base	+pt	+xgb(m)	+pt	+xgb(m, tau)	+pt	Base	+pt	
A	500	15	0.5	1.19	0.93	0.59	<b>0.52</b>	0.73	0.76	0.58	0.88	0.91
	500	15	2.0	0.51	0.43	0.35	<b>0.29</b>	0.43	0.45	0.49	0.40	0.43
	500	30	0.5	0.96	1.04	0.62	<b>0.49</b>	1.13	0.94	0.75	0.79	0.86
	500	30	2.0	0.48	0.48	0.48	<b>0.31</b>	0.44	0.49	0.52	0.34	0.46
	1000	15	0.5	0.46	0.41	0.50	<b>0.36</b>	0.48	0.48	0.53	0.55	0.61
	1000	15	2.0	0.32	0.32	0.28	<b>0.24</b>	0.32	0.30	0.47	0.27	0.35
	1000	30	0.5	0.48	0.64	0.39	<b>0.35</b>	0.51	0.48	0.56	0.44	0.80
	1000	30	2.0	0.34	0.33	0.28	<b>0.26</b>	0.29	0.28	0.46	<b>0.26</b>	0.39
B	500	15	0.5	2.84	2.95	2.77	2.64	3.42	2.97	4.65	2.51	<b>2.48</b>
	500	15	2.0	2.53	2.45	2.20	2.43	2.37	2.34	3.07	2.23	<b>2.10</b>
	500	30	0.5	2.67	2.68	2.66	2.66	2.89	2.76	5.17	2.46	<b>2.45</b>
	500	30	2.0	2.42	2.45	2.32	2.37	2.35	2.37	3.35	2.26	<b>2.12</b>
	1000	15	0.5	2.49	2.49	2.18	2.17	2.32	2.27	3.79	2.05	<b>1.93</b>
	1000	15	2.0	2.30	2.25	<b>1.27</b>	1.29	1.33	1.31	1.96	1.76	1.48
	1000	30	0.5	2.34	2.33	2.23	2.31	2.53	2.32	3.95	2.13	<b>1.96</b>
	1000	30	2.0	2.31	2.33	1.50	1.67	1.58	1.62	2.17	1.92	<b>1.46</b>
C	500	15	0.5	13.48	13.42	12.90	13.52	17.62	16.92	15.02	12.50	<b>12.43</b>
	500	15	2.0	12.98	13.04	10.34	10.38	10.26	10.68	<b>9.83</b>	11.96	11.76
	500	30	0.5	12.74	12.80	12.96	13.21	19.91	19.47	15.15	12.13	<b>12.02</b>
	500	30	2.0	12.89	12.92	11.25	11.39	12.36	12.55	<b>10.70</b>	12.08	11.87
	1000	15	0.5	12.81	12.81	<b>10.61</b>	<b>10.61</b>	13.05	13.55	10.74	11.21	10.96
	1000	15	2.0	12.59	12.64	6.46	6.32	6.28	6.70	<b>6.26</b>	10.16	9.79
	1000	30	0.5	13.09	13.10	11.70	11.69	15.66	15.84	12.35	11.93	<b>11.62</b>
	1000	30	2.0	12.60	12.61	<b>7.74</b>	7.47	7.65	7.75	<b>7.27</b>	10.96	10.07
D	500	15	0.5	5.92	5.91	5.49	5.49	5.66	5.50	5.76	5.41	<b>5.36</b>
	500	15	2.0	5.72	5.71	4.34	<b>4.22</b>	4.25	4.30	4.31	5.22	5.14
	500	30	0.5	5.91	6.03	5.67	5.73	5.90	5.76	6.33	5.75	<b>5.65</b>
	500	30	2.0	5.63	5.54	<b>4.49</b>	4.50	4.51	4.61	4.60	5.32	5.04
	1000	15	0.5	5.68	5.65	4.38	<b>4.31</b>	4.49	4.44	4.64	4.84	4.81
	1000	15	2.0	5.20	5.22	2.65	2.64	<b>2.53</b>	2.68	2.74	4.22	4.03
	1000	30	0.5	5.80	5.70	<b>4.83</b>	5.24	5.06	5.02	5.00	5.25	4.89
	1000	30	2.0	5.21	5.16	<b>2.83</b>	2.85	2.96	2.94	2.95	4.56	4.21